Laser and Particle Beams (2003), *21*, 255–264. Printed in the USA.

DOI: 10.1017/S0263034603212143

The *K*-shell radiation of a double gas puff *z*-pinch with an axial magnetic field

S.A. CHAIKOVSKY, A.YU. LABETSKY, V.I. ORESHKIN, A.V. SHISHLOV, R.B. BAKSHT, A.V. FEDUNIN, AND A.G. ROUSSKIKH

High Current Electronics Institute, Tomsk, Russia

(RECEIVED 1 April 2003; ACCEPTED 16 May 2003)

Abstract

A double shell *z*-pinch with an axial magnetic field is considered as a *K*-shell plasma radiation source. One-dimensional radiation-hydrodynamics calculations performed suggest that this scheme holds promise for the production of the *K*-shell radiation of krypton ($h\nu \approx 12$–17 keV). As a first step in verifying the advantages of this scheme, experiments have been performed to optimize a neon double-shell gas puff with an axial magnetic yield for the *K*-shell yield and power. The experiments show that the application of an axial magnetic field makes it possible to increase the *K*-shell radiation power and reduce the shot-to-shot spread in the *K*-shell yield. Comparisons between the experiments and modeling are made and show good agreement.

Keywords: Axial magnetic field; Implosion stability; *K*-shell radiation source; *Z*-pinch

1. INTRODUCTION

The *z*-pinches accelerated in the diodes of high current generators are now widely used as powerful sources of soft X rays. The spectrum of this type of radiation source ranges from 0.1 to approximately 7 keV. For the production of "harder" X rays (with energies of 20 keV and greater), electron beams interacting with cold condensed targets are employed. Powerful radiation sources operating in the range 7–20 keV are not available nowadays. Ratakhin (1997) compared two types of radiation source (*z*-pinches and electron-beam-based sources) and considered the prospects for using them as a base to create a radiation source operating in the spectral range 7–20 keV. It was shown that only the schemes based on *z*-pinches had a promise for solving this problem.

However, even with the *z*-pinch scheme, the creation of a powerful radiation source for the 7–20 keV spectral range presents a considerable challenge. For a "softer" spectral range, a highly efficient conversion of the kinetic energy of a *z*-pinch into *K*-shell radiation can be achieved. For the elements with a nuclear charge of 10–18 whose *K*-shell radiation falls in the range $h\nu \approx 1$–3 keV, with megaampere current generators, the efficiency may reach several tens percent (Mosher *et al.*, 1999). To generate *K*-shell radiation in the 7–20 keV spectral range, high atomic number materials, such as krypton whose *K*-lines are in the range from 12 to 17 keV, should be used for the working medium. The efficiency of the conversion of the *z*-pinch kinetic energy into *K*-shell radiation decreases substantially with increasing nuclear charge. This decrease can be compensated, in fact, only by increasing the generator current. According to optimistic estimates (Mosher *et al.*, 1999), it is expected that the generation of *K*-shell radiation of krypton might be efficient (about 10–25%) for *z*-pinch currents higher than 40 MA.

However, a multimegaampere generator alone does not make the radiation production efficient. For the elements with a high nuclear charge *Z*, the kinetic processes occurring in plasma, such as the relaxation of the ion charge state, the energy exchange between ions and electrons, the spectral line radiation, and so forth, come to the forefront. Davis *et al.* (1996) used a one-dimensional radiation magnetohydrodynamic (1D RMHD) model to compute the yield of the *K*-shell radiation of krypton during the implosion of a *z*-pinch on a multimegaampere generator. The calculations have shown that the *K*-shell radiation yield for a 40-MA current flowing through the *z*-pinch is 10–50 kJ/cm; that is, the efficiency of the conversion of the kinetic energy of the *z*-pinch into the energy of *K*-shell X rays is low (not over 2%). This is primarily due to the high radiative ability of krypton in the *M*- and *L*-lines. Since a considerable portion of the energy deposited in the pinch is radiated in a "softer"

Address correspondence and reprint requests to: S.A., Chaikovsky, High Current Electronics Institute SD RAS, 4 Akademichesky Ave., 634055 Tomsk, Russia. E-mail: stas@ovpe.hcei.tsc.ru

range, the temperatures necessary for the production of *K*-shell radiation are very difficult to attain.

Another problem which arises in developing *z*-pinch plasma radiation sources (PRSs) is associated with large-scale instabilities which inevitably develop in an imploding *z*-pinch. This is especially critical for a PRS which radiates in the hard spectral range, since in this case the need to use high-*Z* materials dictates the necessity to start an implosion from a large initial radius. To overcome the ionization barrier and to heat the plasma to a temperature at which the *K*-shell electrons of krypton radiate efficiently, the final implosion rate should be no less than 10^8 cm/s (Whitney *et al.*, 1990). To attain these values even on a generator with a current rise time of 100 ns, it is necessary that the initial radius of the *z*-pinch be no less than 3 cm. The available experimental and calculation data suggest that *z*-pinch implosions starting from large initial radii ($>$ 3 cm) are very unstable (Baksht *et al.*, 1995; Coleman *et al.*, 1997; Commisso *et al.*, 1998; Cochran, Davis & Velikovich, 1995). It should be emphasized that an increase in initial *z*-pinch radius is also dictated by the increase of the rise time of the generator current, which seems to be unavoidable in the future multimegaampere generators. Therefore, to create an efficient *z*-pinch-based source radiating in the range from 7 to 20 keV, it is necessary to take additional measures to stabilize the implosion process.

This article considers the possibility of using a double-shell gas puff with an axial magnetic field to produce high-power pulsed radiation with a photon energy of 7–20 keV. A similar scheme was considered (Gol'berg, Liberman & Velikovich, 1990) as a candidate for use in realizing inertial confined fusion. In this scheme, the inner shell is a solid gas column (solid fill) and the outer shell is an annular gas shell with an axial magnetic field inside. The implosion stability is provided by the axial magnetic field. One-dimensional hydrodynamic calculations performed for a multimegaampere generator with a 300-ns current rise time, which are discussed in Section 2 of this article, suggest that this scheme holds promise for the production of the *K*-shell radiation of krypton. In the case of a krypton pinch, the role of the magnetic field is not limited to implosion stabilization. According to the predictions, the magnetic field reduces the radiative energy losses in the soft spectral range and thus makes the heating of the plasma more efficient.

An implosion experiment with Kr double gas puffs in the presence of an axial magnetic field on a multimegaampere (40–60 MA) generator is still costly and a long way in the future. Therefore, a contemporary problem to be solved is to study the efficiency of the production of *K*-shell radiation using this *z*-pinch scheme on available generators of lower current level, and, hence, for lower atomic number elements. Of particular interest is this type of experiment with long ($>$ 100 ns) rise times of the generator current. This is due to the fact that the trend is to longer current rise times in multimegaampere generators. The generators with a long current rise time seem to be less complicated in design and their cost is lower in comparison with the generators whose current rise time is 100 ns or shorter.

The experiments under discussion in this article were performed with double gas puff *z*-pinches and an axial magnetic field on the IMRI–5 generator producing a current of 400 kA with a rise time of 430 ns. Neon was used for the working gas. The gas-puff parameters were chosen using preliminary one-dimensional RMHD calculations. The experiments were aimed, first, at investigating the effect of an axial magnetic field on the stability, power, and yield of the *K*-shell radiation of a double gas puff with a solid inner shell at long implosion times ($>$ 100 ns) and, second, at checking whether the model description of an imploding gas puff with an axial magnetic field is adequate.

The article is organized as follows. In Section 2, the advantages of the B_Z double gas puff scheme are considered and the results of the preliminary 1D RMHD simulation are given. The experimental setup and diagnostics used in the experiments are described in Section 3. The experimental data are presented in Section 4 and the results are discussed in Section 5. The principal results of the research are summarized in Section 6.

2. PREDICTIONS OF THE NUMERICAL SIMULATION

The configuration used in our experiments is shown in Figure 1. The inner shell is a solid gas column (solid fill), while the outer shell is an annular gas shell with an axial magnetic field inside. The application of an axial magnetic field is the well-known method for stabilizing plasma *z*-pinch implosions. Stabilization of the shell could occur during the run-in phase of implosion due to the compression of the magnetic field frozen in the plasma (Rudakov, 1989). In experiments with single and double gas puffs, the magnetic field used made the implosion much more stable (Sorokin & Chaikovsky, 1989, 1993). The initial magnetic field necessary to produce a compact and uniform *z*-pinch was $B_0 = (0.5\text{–}1)B_{st}$. Here, $B_{st}\,(\text{kG}) = 10I_{max}\,(\text{MA})/R_0\,(\text{cm})$ is the low-

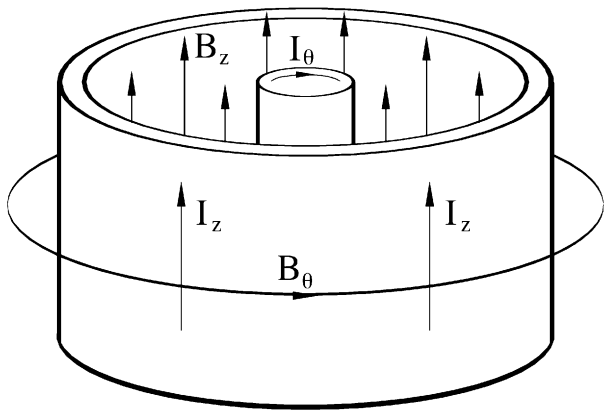

Fig. 1. Double-shell gas puff with an axial magnetic field.

https://doi.org/10.1017/S0263034603212143 Published online by Cambridge University Press

est magnetic field at which the implosion of an annular gas shell is still stable (Bud'ko *et al.*, 1989; Sorokin & Chaikovsky, 1989), were I_{max} is the maximum current through the gas shell and R_0 is the initial radius of a single gas puff or the initial radius of the outer shell of a double gas puff.

An advantage of a solid inner shell is the snowplow stabilization mechanism (Gol'berg & Velikovich, 1993) that works when the shell matter is swept during the propagation of the shock wave. When the inner shell of a gas puff is a solid fill, the shock wave propagates in the matter almost until the moment of maximum compression; therefore, the snowplow stabilization may have a substantial effect.

Early in the process, the generator current flows in the outer shell and accelerates the latter. If the conductivity of the shells is high enough, then, as the outer shell implodes, the axial magnetic field trapped between the shells is compressed. The inner shell is accelerated both by the action of the azimuth currents, which appear because of the axial magnetic field compression between the shells, and by the action of the gas-dynamic pressure. In this case, the time of acceleration of the inner shell is determined by the time of collision of the shells, and it is considerably shorter than the generator current rise time. Therefore, the energy transfer to the inner shell occurs with an increased power. The material of the inner shell matter is heated to high temperatures at comparatively weak compression by the action of a strong shock wave. When the shock wave arrives at the axis, a reflected shock wave forms, and further implosion of the *z*-pinch is accompanied by a series of shock waves of lower intensity, which pass through the material of the inner shell (Oreshkin, 1995). This has the result that the inner shell appears to be heated to a higher temperature than the outer shell; therefore, the contribution of the inner shell to the radiation in the "hardest" spectral range is more substantial than that of the outer shell.

Let us consider the simulation predictions for the krypton *K*-shell radiation yield produced by a double gas puff with an axial magnetic field used for the load of a multimegaampere generator. The lumped circuit of the generator is shown in Figure 2a. The generator circuit has the following parameters: $U(t) = U_0 \sin(\pi t/2\tau_0)$, $U_0 = 12$ MV, $\tau_0 = 250$ ns, $R = 0.185$ Ω, $L = 12$ nH. Figure 2b shows the short-circuit current and the load current calculated for an imploding double-shell gas puff. The generator power is about 200 TW and the stored energy is estimated to be 70–80 MJ. The *z*-pinch implosion was simulated with the use of a one-dimensional two-temperature magnetohydrodynamic code (Oreshkin, 1994). This code employs the one-dimensional two-temperature radiation magnetohydrodynamics equations. The following dissipation processes are included in the model: electron and ion heat conductivity, Ohmic heating (for the Spitzer conductivity), interchange of energy between ions and electrons, and radiation losses. The dissipation process coefficients were taken in the frame of a Braginskii model (Braginskii, 1965). The pseudo-viscous pressure was employed in the code for the calculation of the

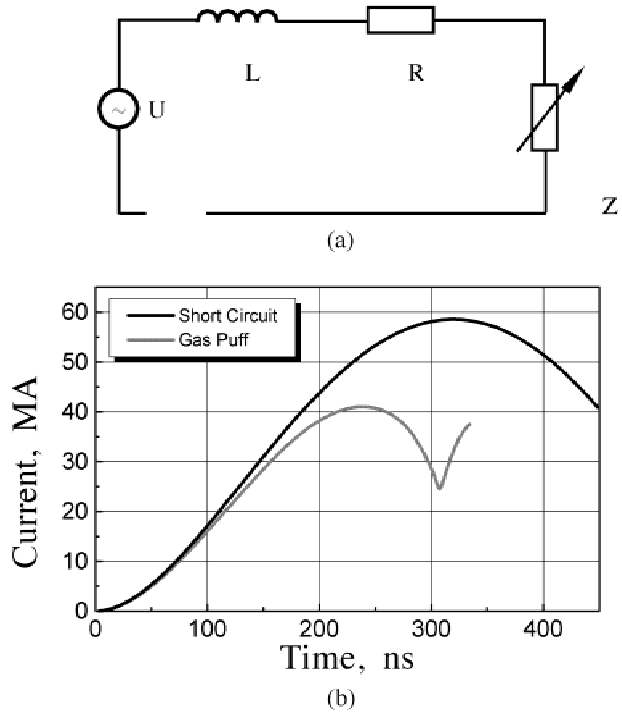

Fig. 2. Lumped circuit of 60-MA generator (a) and calculated current traces (b) for a case of short-circuit load and a double shell gas puff.

shock-wave front. The collision-radiative model was used for computing of the radiation losses and the plasma ionization states. It takes into account the following elementary processes: electron collisional excitation; spontaneous and stimulated emission; collisional and photoionization; and collisional, radiative, and dielectronic recombinations. For the calculation of plasma ionization states, the quasi-steady approach was used in the model, that is, the plasma ionization states were found by solving time-dependent equations of ionization dynamics, while the population density was determined by solving the stationary rate equation, since the relaxation time of the excited ion levels is considerably less than the ionization state relaxation time.

The simulations were performed for double gas puffs by varying the initial radius of the outer shell R_{out} so that the ratio $R_{in}/R_{out} = 0.2$ was preserved. Here, R_{in} is the initial radius of the inner shell. The gas puff length was 5 cm. The gas puff mass was chosen so that the *z*-pinch implodes at a nearly peak load current. The inner-to-outer-shell mass ratio remained unchanged: $m_{in}/m_{out} = 0.5$. The initial value of the axial magnetic field was varied so that the stabilization criterion $B_0 = B_{st}$ was satisfied. The predicted dependence of the Kr *K*-shell yield on the initial outer shell radius is shown in Figure 3. It can be seen that with the given generator a double-shell gas puff with an axial magnetic field is capable of producing a *K*-shell yield of up to 300 kJ/cm. This value is close to the highest possible yield predicted by the simplified estimates using a model of Mosher (Mosher *et al.*, 1999) and is substantially greater than that predicted by Davis *et al.* (1996).

https://doi.org/10.1017/S0263034603212143 Published online by Cambridge University Press

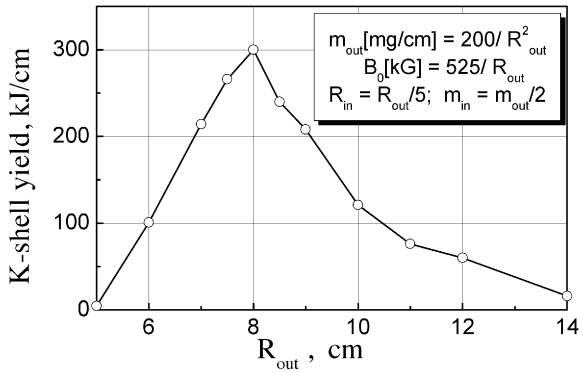

Fig. 3. Calculated dependence of the Kr *K*-shell radiation yield on the initial radius of the outer shell of the B_Z double gas puff.

An important feature of the scheme under consideration is that the axial magnetic field not only stabilizes the gas puff implosion. The magnetic field prevents a *z*-pinch plasma from excessive compression that leads to the large radiation losses in the soft spectral range and does not allow obtaining conditions required for *K*-shell radiation generation. Simulations carried out for the case with no magnetic field have shown that, when compressed to the same degree as with a magnetic field, the plasma is not heated to the required temperature and the *K*-shell yield is negligibly low.

Thus, the key idea of the proposed method is to choose the gas puff initial density profile and the axial magnetic field so that the resulting implosion dynamics would provide the heating of the plasma to a temperature sufficient for the production of *K*-shell radiation at a comparatively low plasma density. This should reduce the energy losses by soft radiation as the gas puff goes through the "radiation barrier" and, hence, increase the energy available for the emission of *K*-shell radiation at the final stage of implosion. Evidently, this approach carries a kind of compromise. On the one hand, if there is an axial magnetic field, there should be energy losses for its compression and a decrease in the energy delivered to the plasma. However, in this case, the radiative losses in the soft spectral region decrease. As a result, according to the simulations, the plasma temperature can reach values necessary for the generation of Kr *K*-shell radiation. On the other hand, if there is no magnetic field, the plasma cannot be heated to the required temperature because of the substantial radiative energy losses in the soft spectrum.

As mentioned above, the method under consideration cannot be verified experimentally on a multimegaampere generator, in particular, because generators of this type are not available at present. However, the key aspects of this scheme, such as the implosion stability and the efficiency of the conversion of the generator energy into *K*-shell radiation in the presence of a magnetic field can be investigated experimentally on the now available generators producing lower currents for low-*Z* materials. It should however be noted that the fraction of the radiative losses associated with the soft spectral region in the plasma energy balance decreases substantially with decreasing the nuclear charge. Therefore, the effect of the magnetic field upon the *K*-shell radiation power and yield for low-*Z* materials can be negative. Experiments show that, notwithstanding an improvement in implosion stability with increasing the initial magnetic field, the radiation power and yield decrease both in the spectral region < 1 keV (Sorokin & Chaikovsky, 1989) and in the spectral region > 1 keV (Sorokin & Chaikovsky, 1996). Obviously, this is due to the energy losses for the compression of the axial magnetic field. Takasugi et al. (2000) used a longitudinal magnetic field to suppress the *K*-shell radiation of argon.

Prior to the experiment on the IMRI-5 generator, preliminary RMHD calculations of the Ne *K*-shell ($h\nu \approx 0.9$–1.4 keV) radiation yield had been performed for a double-shell gas puff with an axial magnetic field. The neon gas was chosen because a measurable *K*-shell yield was expected at IMRI-5 generator current level. In the calculations, the peak current was 600 kA and the current rise time was 450 ns. The goal of these calculations was to determine optimum outer and inner shell parameters (radii and masses) for maximizing the Ne *K*-shell radiation yield. Figure 4 shows the calculated dependence of the Ne *K*-shell radiation yield on the outer shell radius for a B_Z double gas puff of length 2 cm. In the simulations, the gas puff mass was varied so that the implosion occurred at a nearly maximum of load current, and the initial value of the axial magnetic field was set so that the stabilization criterion $B_0 = B_{st}$ was satisfied. As can be seen in Figure 4, the maximum radiation yield in the simulations was predicted for the outer shell radius equal to 3.5 cm; therefore, the *K*-shell yield dependences on the inner shell mass and radius were calculated for this value of the outer shell radius.

The calculations, the results of which are presented in Figure 5, were carried out for a constant value of the inner shell radius (at inner-to-outer shell radii ratio $R_{in}/R_{out} = 0.2$) in one case and for a constant value of the gas puff mass (at inner-to-outer shell mass ratio $m_{in}/m_{out} = 0.5$) in the

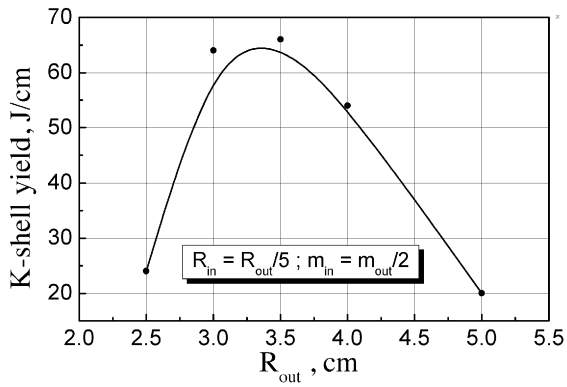

Fig. 4. Calculated dependence of the Ne *K*-shell radiation yield on the outer shell radius of the B_Z double gas puff for the conditions of the IMRI-5 generator.

https://doi.org/10.1017/S0263034603212143 Published online by Cambridge University Press

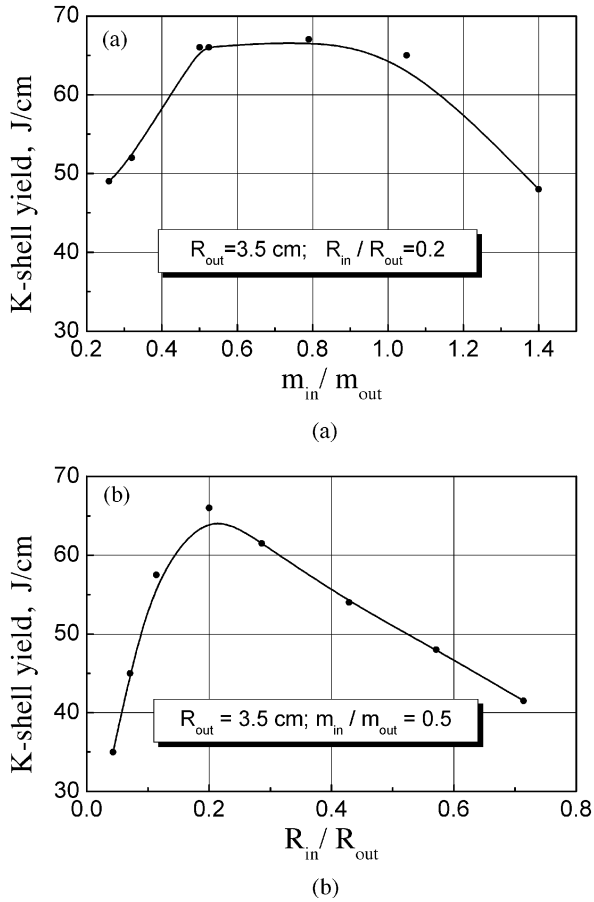

Fig. 5. The Ne *K*-shell radiation yield versus the shell mass ratio (a) and the shell radius ratio (b) of the B_Z double gas puff on the IMRI-5 generator.

other. The calculation allows us to conclude that the ratios of the shell parameters optimized for the production of the highest possible *K*-shell yield are as follows: $R_{in}/R_{out} = 0.2$–0.25 and $0.5 \leq m_{in}/m_{out} < 1$.

3. EXPERIMENTAL EQUIPMENT AND DIAGNOSTICS

The experiments were carried out on the IMRI-5 generator, which is a low-inductance capacitor bank with a capacitance of 3.23 μF. With a charge voltage of 75 kV, the capacitor bank stores 9 kJ. In the short-circuit regime, the generator provides a peak current of 470 kA with a current rise time of 430 ns. Neon gas puffs were formed by pulsed injection of the gas through supersonic nozzles into the electrode gap of the generator. The distance between the anode and the cathode was either 1.7 cm or 2.2 cm (for the nozzle configuration 100/20). To produce double gas puffs with different initial radii, we used interchangeable nozzles with the Mach 4–6. The nozzle parameters are listed in Table 1. The outer nozzles had an 8° inward tilt (see Fig. 6) to reduce the zipper effect in gas puff implosions. In all nozzle configurations, the outer shell was an annular gas puff, while the inner shell was a solid fill.

Table 1. *Nozzle parameters*

Nozzle configuration	Mean diameter of the outer nozzle, cm	Outer diameter of the inner nozzle, cm
44/10	4.4	1.0
60/12	6.0	1.2
80/16	8.0	1.6
100/20	10.0	2.0

During the experiments, the shell masses were adjusted by varying the gas valve plenum pressure and the time delay between the gas valve opening and the generator firing. To estimate the shell masses, additional sets of experiments were performed for each nozzle configuration without an axial magnetic field both with the outer shell alone and with the inner shell alone. The implosion times were determined using the signals from magnetic probes, XRDs, and Rogowski coils. Then the implosions of the gas puffs were simulated with the help of the snowplow model using the current traces obtained in the experiments. For each shot, the iteration calculations, where the initial gas puff mass was varied, were carried out until the calculated implosion time coincided with the implosion time observed in the experiments.

For the preionization of a gas puff, we used a flashboard, whose operation is based on a discharge over a dielectric surface. The axial magnetic field was created by two magnetic coils.

In the experiments with neon double gas puff, the following diagnostics complex was used. The load current was measured by a Rogowski coil that was located in the return current lead (see Fig. 6). The Ne *K*-shell ($h\nu \approx 0.9$–1.4 keV) radiation power and yield were measured by two vacuum X-ray diodes (XRD) with aluminum cathodes and the following filters: aluminum 10 μm + Mylar 3 μm (XRD1) and aluminum 0.6 μm + Kimfoil 6 μm (XRD2). Two pinhole cameras were fielded to record the time-integrated image of the pinch. One pinhole camera was filtered by 8-μm-thick aluminum foil and the other was placed behind a filter of aluminum 0.2 μm + Kimfoil 2 μm. The implosion dynamics was recorded by a visible light streak camera with a

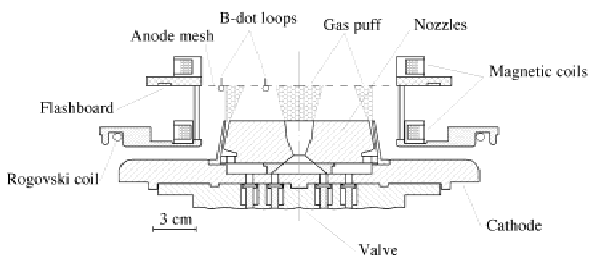

Fig. 6. Schematic drawing of the IMRI-5 generator load unit with 100/20 nozzle configuration.

https://doi.org/10.1017/S0263034603212143 Published online by Cambridge University Press

writing speed of 125 ns/cm. The inlet slit of the streak camera was arranged perpendicular to the *z*-pinch axis.

4. EXPERIMENTAL RESULTS

The general experimental procedure was the following. At the first stage of the experiments, the outer shell mass at which the implosion time was in the interval 450–480 ns (i.e., approximately equal to the generator current rise time) was determined for each nozzle configuration. At the second stage, with the outer shell mass kept equal to the found optimum value, the *K*-shell radiation power and yield were measured at different masses of the inner shell that was varied by changing the plenum pressure in the corresponding gas-valve volume. Thus, the optimum inner shell mass with respect to *K*-shell radiation production and the maximum *K*-shell yield were found for the double-shell gas puff without an axial magnetic field. At the next stage, the *K*-shell yield was measured as a function of the initial axial magnetic field for the optimum inner and outer shell masses determined in the preceding stage of the experiments. The value of the initial magnetic field was varied in the range (0.3–1.5) B_{st}. Finally, an additional scan on the inner shell mass was carried out for the double gas puff with the axial magnetic field that was chosen in the course of the previous stage of experiments.

Table 2 presents the values of shell masses, *K*-shell radiation yield and power, and final implosion velocity for the shots in which a maximum *K*-shell radiation yield was registered for each configuration with a magnetic field $B_0 \approx 0.5B_{st}$. The experiments have shown (see Table 2) that the configuration with 6 cm outer diameter (60/12 configuration) is an optimum for the generation of *K*-shell radiation.

The experimental data on the *K*-shell radiation power and yield obtained for this configuration are presented in Figure 7. Figure 7a shows the dependence of the Ne *K*-shell radiation yield and power on the inner shell mass in the experiments without an axial magnetic field. The maximum *K*-shell radiation yield, 63 J/cm, has been fixed for the inner shell mass equal to 7.5 ± 2 μg/cm. The mass of the outer shell in these experiments was 12 ± 5 μg/cm, providing the implosion time in the interval from 435 to 540 ns. Figure 7b illustrates the dependence of the *K*-shell radiation yield and power on the initial axial magnetic field. The mass of the inner shell in these shots was in the range 5–7.5 μg/cm. The maximum value of the *K*-shell radiation yield for the initial magnetic field B_0 = 0.66 kG is equal to 48 J/cm, which is 30% lower than the maximum *K*-shell yield measured in the experiments without magnetic field. The average *K*-shell yields for these two cases are comparable.

In the double gas puff implosions, the *K*-shell radiation power increases with axial magnetic field. The maximum *K*-shell power measured for B_0 = 0.66 kG is 4 GW/cm, which is twice that measured in the shots without the axial magnetic field. The dependence of the *K*-shell radiation yield and power on the inner shell mass for the optimum value of the initial magnetic field is shown in Figure 7c. It can be seen that the *K*-shell yield has a maximum when the inner shell mass is 5 ± 1.5 μg/cm.

An increase in initial magnetic field reduced the shot-to-shot spread in radiation yield (see Table 3). With the practically equal average values of the *K*-shell yield in the shots with B_0 = 0 kG and B_0 = 0.66 kG, the dispersion of the

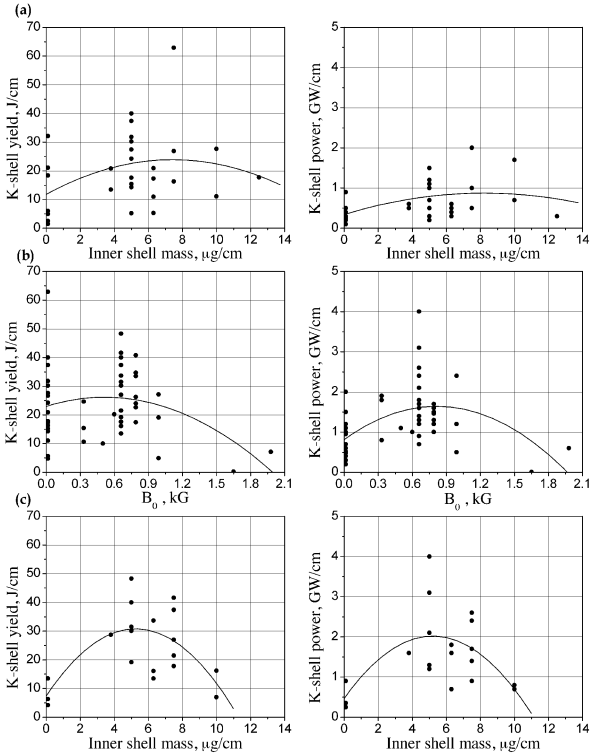

Fig. 7. Nozzle configuration 60/12. Ne *K*-shell radiation yield and power in the experiments with double gas puff (a) without an axial magnetic field, (b) with an axial magnetic field at the constant gas puff mass, and (c) with the axial magnetic field (B_0 = 0.66 kG) at varying mass of the inner shell.

Table 2. *The gas puff parameters, the implosion velocity, and the maximum K-shell radiation yield and power*

D_0, cm	m_{out}, μg/cm	m_{in}, μg/cm	B_0, kG	Y_k, J/cm	P_k, GW/cm	V_f, 10^7 cm/s
4.4	17 ± 3	2 ± 1	0	5.5	0.2	2.0
6	14 ± 5	7.5 ± 2	0	63	2	1.85
8	5 ± 1	17 ± 5	0	38	2.9	1.4
10	2.5 ± 1	27 ± 8	0	32	0.8	—
4.4	20 ± 3	1.5 ± 1	0.77	1	0.1	2.7
6	11 ± 5	5 ± 2	0.66	48.5	4	2.25
8	5 ± 1	17 ± 5	0.55	28.5	1.7	1.6
10	2.5 ± 1	27 ± 8	0.49	4	0.2	1.1

Notation: D_0: the outer shell initial diameter (the external diameter of the inner shell was equal to 0.2 D_0 in all shots), m_{out}: the outer shell mass, m_{in}: the inner shell mass, B_0: the induction of the initial axial magnetic field, Y_k: the Ne *K*-shell radiation yield, P_k: the Ne *K*-shell radiation power, and V_f: the implosion velocity estimated from streak camera pictures.

https://doi.org/10.1017/S0263034603212143 Published online by Cambridge University Press

Table 3. *The average K-shell yield, Y_{kav}, and the standard deviation D of Y_k values from an average value at optimum inner shell mass for different values of the initial magnetic field B_0*

Nozzle configuration	B_0, kG	Y_{kav}, J/cm	D, J/cm	D/Y_{kav}, %
60/12	0	35.4	24.7	70
60/12	0.66	33.8	10.6	31
80/16	0	22.9	13.8	60
80/16	0.39	19.8	8.8	44
80/16	0.55	19.7	5.9	30

experimental points about the average value in the later case is less by half.

Figure 8 shows time-integrated pinhole images and streak camera pictures for the implosion of a double gas puff with the inner shell mass equal to 7.5 μg/cm for a varied initial magnetic field. The final implosion velocity estimated from the streak camera pictures was $(1.4–1.7)\cdot10^7$ cm/s. The presence of an axial magnetic field significantly improves the implosion stability. At the initial axial magnetic field $B_0 = 0.66$ kG (that is $\approx 0.5B_{st}$ for 60/12 configuration) the final plasma column becomes quite uniform along the *z*-axis. The diameter of the *z*-pinch radiating in Ne *K*-lines is practically the same in the shots with $B_0 = 0$ kG and $B_0 = 0.66$ kG. Time-integrated pinhole images and streak camera pictures of the *z*-pinch implosions without the axial magnetic field are shown in Figure 9. It can be seen that an imploding single gas puff (without an inner shell) does not produce a compact uniform pinch. An increase in the inner shell mass improves the radial and axial uniformity of the pinch. Comparing Figure 8 and Figure 9, we can see that the pinch produced by the imploded double-shell gas puff with an axial magnetic field was more uniform.

Thus, with the given nozzle configuration, the application of an axial magnetic field not only improved the double gas puff stability, but also increased the *K*-shell power with comparable *K*-shell radiation yields.

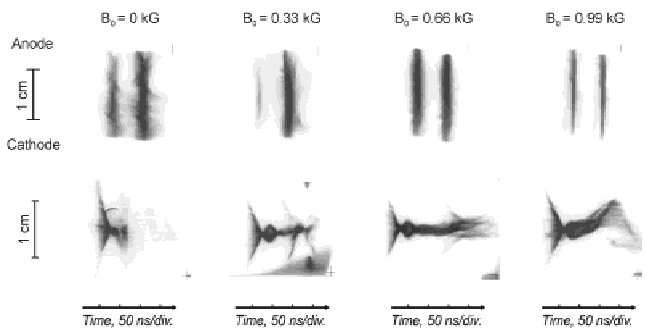

Fig. 8. Time-integrated pinhole images and streak camera pictures obtained at different values of the initial axial magnetic field (in the pinhole camera pictures: the pinch image in Ne *K*-lines—at the left, the pinch image in soft X rays—at the right).

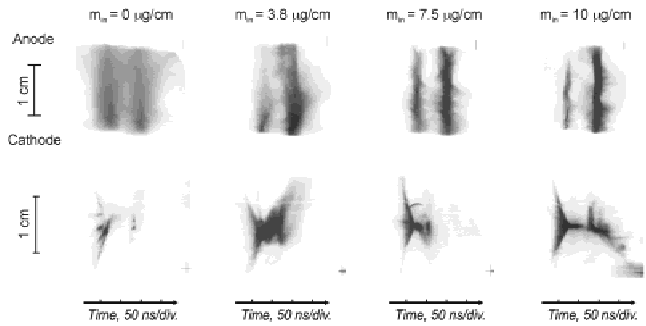

Fig. 9. Time-integrated pinhole images and streak camera pictures obtained at different values of the inner shell mass in the shots without the axial magnetic field (in the pinhole camera pictures: the pinch image in Ne *K*-lines—at the left, the pinch image in soft X rays—at the right).

The higher implosion velocities realized in the shots with an axial magnetic field (see Table 1) are accounted for by the experimentally observed decrease in implosion time in the presence of a magnetic field. In the shots with an axial magnetic field, the implosion time was 40–60 ns (~10%) shorter compared to the shots without a magnetic field (Fig. 10). The decrease in implosion time in the presence of an axial magnetic field was observed for all nozzle configurations used in the experiments.

5. DISCUSSION OF THE EXPERIMENTAL RESULTS

When discussing the experimental results, we will invoke the results of 1D RMHD calculations. In Section 2, the results of preliminary calculations of the Ne *K*-shell yield from a B_Z double gas puff PRS on the IMRI-5 generator were presented. However, the conditions for which these calculations were carried out were somewhat different from the experimental conditions. Therefore, we performed additional calculations for the maximum load current and the

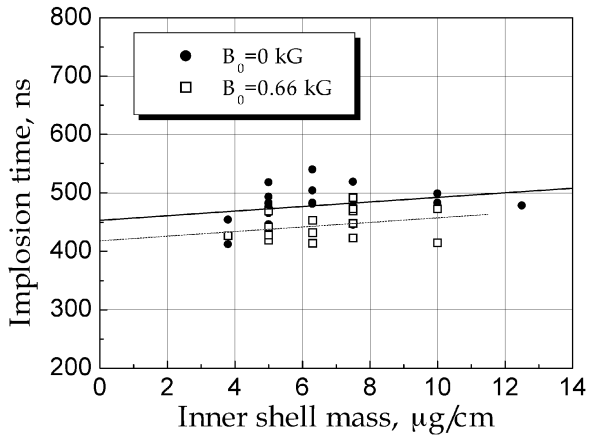

Fig. 10. Dependence of the implosion time on the inner shell mass of the double gas puff in the experiments with and without the axial magnetic field.

https://doi.org/10.1017/S0263034603212143 Published online by Cambridge University Press

shell masses close to those realized in the experiment. In these calculations, the shell masses were chosen so that, on the one hand, they corresponded (within the experimental error) to the experimental values and, on the other hand, the implosion time in the simulations was about 500 ns, as in the best shots. Moreover, in the preliminary calculations, the magnetic field was set equal to B_{st} in compliance with the lower limit specified by the condition for magnetic-field-stabilized implosions. The experiments, however, have shown that for a double-shell gas puff, stabilization is attained with a magnetic field equal to $0.5B_{st}$.

The experimental and calculated *K*-shell yields are shown in Figure 11 as a function of the outer shell diameter for the initial magnetic field $B_0 \approx 0.5B_{st}$. The experimental points correspond to the best shots in each nozzle configuration with the respective maximum *K*-shell radiation yield. Recall that for all configurations the inner-to-outer shell radius ratio was approximately constant and satisfied the condition obtained in the preliminary calculations: $R_{in}/R_{out} \approx 0.2$–$0.25$.

As can be seen in Figure 11, both in the experiments and in the simulations the maximum *K*-shell yield corresponded to the initial outer shell diameter equal to 6 cm. It should be noted that the optimum diameter of the outer shell was determined with sufficient accuracy in the course of the preliminary 1D RMHD simulations (see Fig. 4).

The maximum yields achieved experimentally are greater than the maximum yield for a single shell gas puff by a factor of 1.5–2 and are close to the values that can be realized on a generator with the same current, but with shorter implosion times (≈100 ns). Indeed, when optimizing the *K*-shell yield for single shell gas puffs, we have shown that the *K*-shell yield has a maximum of 30 J/cm at the initial shell diameter equal to 6 cm. Estimation of the *K*-shell yield for a single shell gas puff performed with a two-level model (Mosher *et al.*, 1999) for a generator producing currents on the level of the IMRI-5 currents with a current rise time of 100 ns gives a value 74 J/cm.

The experimental and calculated dependences of the Ne *K*-shell yield and power on the initial axial magnetic field for 60/12 configuration are shown in Figure 12. It can be seen that the calculated and experimental yields are in good qualitative and quantitative agreement. As the magnetic field was increased to 0.66 kG, both the calculated and the experimental yield changed insignificantly. From Figure 8, which presents integrated pinhole images of a *z*-pinch for different values of the initial axial magnetic field, it can be seen that as the initial axial magnetic field is increased, the final plasma column becomes more uniform along the *z*-axis, that is, unstable modes with $m = 0$ are more suppressed. When the magnetic field is over 0.66 kG, along with a further increase in stability, both the calculated and the experimental *K*-shell yield are observed to decrease.

As can be seen in Figure 12b, for the experimental values of the *K*-shell radiation power there is a pronounced maximum at the initial value of the axial magnetic field equal to 0.66 kG. As the magnetic field is increased, the power decreases because of the increase in the energy lost for the compression of the magnetic field. With decreasing magnetic field, the radiation power decreases as well, and this seems to be associated with the influence of large-scale instabilities on the *z*-pinch formation at the final stage of implosion. In the absence of an axial magnetic field, the

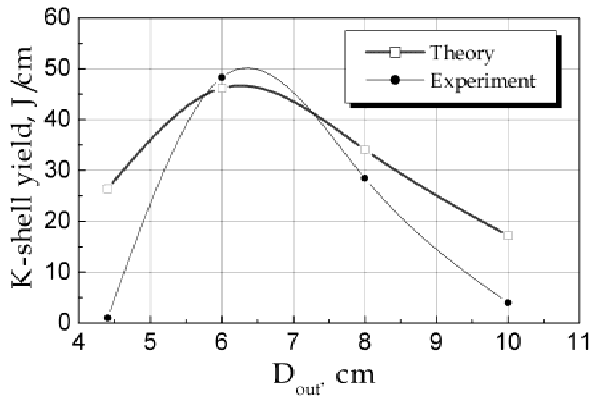

Fig. 11. Experimental and calculated *K*-shell radiation yield as a function of the outer shell diameter of the double gas puff.

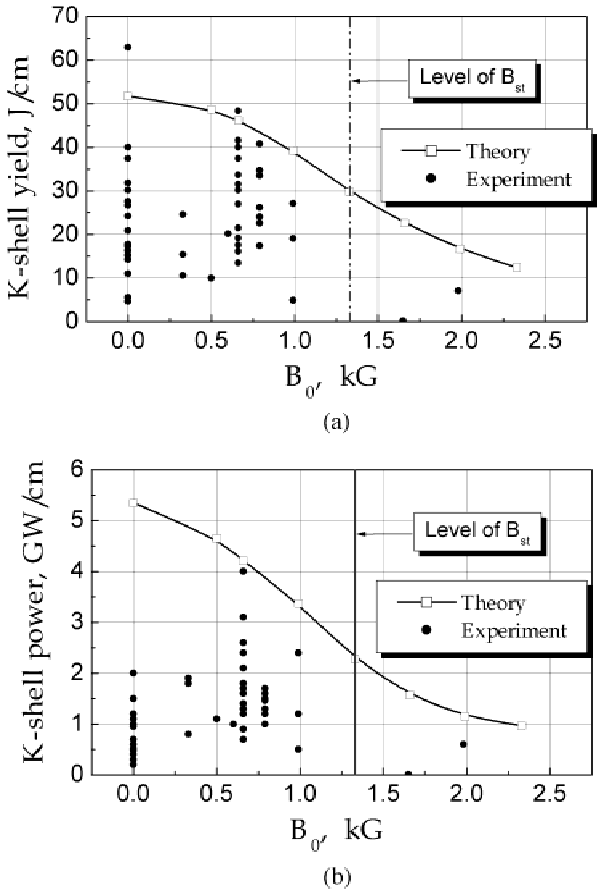

Fig. 12. Ne *K*-shell radiation yield (a) and power (b) as a function of the initial axial magnetic field. Comparison of the experimental and 1D RMHD simulation results.

https://doi.org/10.1017/S0263034603212143 Published online by Cambridge University Press

K-shell radiation power is lower by a factor of 1.5–2.5 compared to its maximum value.

Comparing XRDs waveforms (Fig. 13a), one can see that the duration of the *K*-shell radiation pulse for an imploding double-shell gas puff without an axial magnetic field is substantially longer than that for an imploding double-shell gas puff in the presence of an axial magnetic field. This seems to be due to the fact that different parts of the pinch implode to the axis nonsimultaneously, which is caused by the development of large-scale instabilities in the absence of an axial magnetic field.

Figure 13b compares the experimental and calculated traces of the load current and the XRD response for the case of a double gas puff with an axial magnetic field of 0.66 kG. The experimental current coincides very closely with the calculated one, and the absolute values of the *K*-shell radiation power and pulse width are in a good agreement as well. Note that, according to the simulations, the implosion dynamics of a double gas puff with the initial axial magnetic field corresponding to the criterion $B_0 > B_{st}$ is only slightly different from that without a magnetic field. In experiments, however, the presence of an axial magnetic field results in a 10–15% decrease in implosion time for practically identical initial parameters of the gas puff (see Fig. 12a and Fig. 10). We have yet found no explanation for this effect. It is important that our attempts to optimize the *K*-shell radiation yield in the absence of the axial magnetic field by decreasing the outer shell mass and accordingly decreasing the implosion time did not lead to an increase in *K*-shell yield.

The distributions of the calculated thermodynamic parameters of the plasma at the instant the *K*-shell radiation power peaks are presented in Figure 14. It can be seen that the plasma region with a temperature of 0.2 keV that radiates intensely in the Ne *K*-lines has a rather large radial dimension: Its diameter is 1.4–1.6 mm. The density of this plasma is relatively low, $5\cdot10^{18}$–$1.5\cdot10^{19}$ cm^{-3}, and it is quite uniform, without large gradients of the thermodynamic parameters. The plasma intensely radiating in the Ne *K*-lines consists of the material of the inner shell. Though the material of the outer shell has a higher density, its temperature is significantly lower. Comparing Figure 14 and the corresponding pinhole image (Fig. 8, $B_0 = 0.66$ kG), one can see a very good agreement between the observed and the calculated radial dimensions of the radiating regions.

A set of the experiments has been performed with nozzle configuration 60/12 where the inner solid-fill shell was replaced by an annular shell with the same outer diameter. The above two configurations are almost identical in respect to the energy delivered to the imploding *z*-pinch, since the peak currents, the implosion times, and the final pinch diameters in Ne *K*-lines were practically the same. Nevertheless, in the experiments with an annular inner shell, the maximum *K*-shell yield was lower by a factor of 1.7 in the shots without an axial magnetic field and by a factor of 2.6 in the shots with an axial magnetic field of 0.66 kG compared to that realized for a double gas puff with a solid inner shell. The decrease in *K*-shell yield in the case of an annular inner shell can be explained as follows. After the passage of the first shock wave through the material of the inner shell, the plasma density is higher by a factor of 1.8–2 for the annular inner shell compared to that the solid inner shell. Since the electron temperature at this moment is not high enough to produce *K*-shell radiation, the radiation losses occur mainly in the softer X rays and are greater for the annular shell than for the solid one. Hence, at the final stage of implosion, the energy of the annular shell should be lower. To verify this assumption, 1D RMHD simulations of the

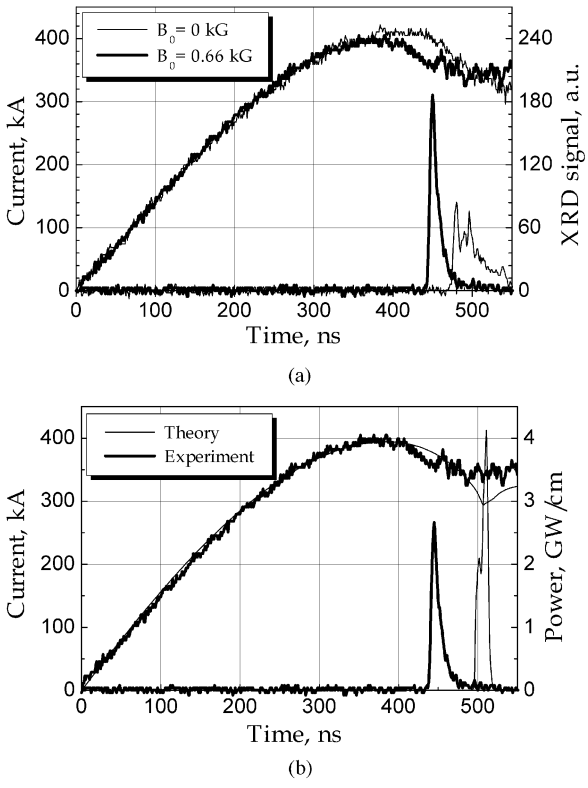

Fig. 13. Load current and XRD traces: (a) comparison of the double gas puff implosions with and without an axial magnetic field; (b) comparison of the experimental and calculated traces of the double gas puff implosion at the initial axial magnetic field of 0.66 kG.

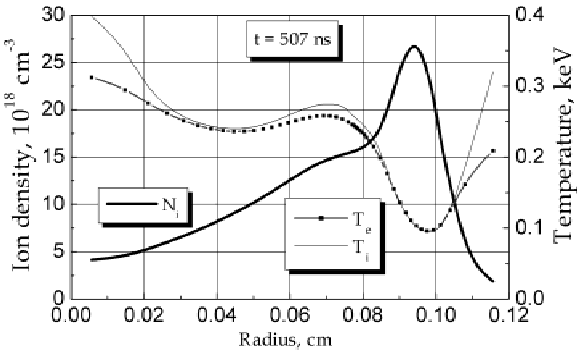

Fig. 14. Distributions of the plasma thermodynamic parameters at the moment of maximum *K*-shell radiation power for the case of double gas puff implosion with the initial axial magnetic field of 0.66 kG.

https://doi.org/10.1017/S0263034603212143 Published online by Cambridge University Press

implosion of a double gas puff with an annular inner shell in the presence of an axial magnetic field have been performed. Actually, these simulations have predicted a somewhat lower *K*-shell yield, but only by 10–15%, against a factor of 2.6 obtained in experiments. This suggests that there must be another reason for the decrease in *K*-shell yield in the experiment with a hollow inner shell. This, perhaps, may be the fact that the implosion dynamics of the inner shell realized in experiment varies with the initial density distribution.

6. CONCLUSION

The 1D RMHD calculations performed have shown that a promising scheme for the production of high-power pulsed *K*-shell radiation in the spectral range 7–20 keV on a multimegaampere generator with a current rise time of 300 ns is a double-shell gas puff *z*-pinch with a solid inner shell and an axial magnetic field. The magnetic field not only provides for implosion stability, but also reduces the radiative energy losses in the soft region, thereby increasing the energy available to produce the radiation in the spectral range 7–20 keV.

As a first step in verifying the advantages of this scheme over conventional single shell gas puffs, experiments have been performed to optimize a neon double-shell gas puff with an axial magnetic field for the *K*-shell yield and power. The IMRI-5 generator used in these experiments produced a peak current of 400 kA with a current rise time of 430 ns.

It has been demonstrated that the application of an axial magnetic field improves the *z*-pinch uniformity for implosion times ranging from 450 to 500 ns. The value of the axial magnetic field sufficient to stabilize the implosion is determined by the criterion: $B_0\,[\mathrm{kG}] \geq 5 I_{max}\,[\mathrm{MA}]/R_0\,[\mathrm{cm}]$.

Optimum parameters of a double gas puff with an axial magnetic field have been found that provide both implosion stability for implosion times of 450–500 ns and the *K*-shell yield comparable with the expected *K*-shell yield on a generator with a current rise time of 100 ns.

The application of an axial magnetic field makes it possible to increase the *K*-shell radiation power and reduce the shot-to-shot spread in the *K*-shell yield.

It has been shown that 1D RMHD calculations are applicable to describe gas puff implosions under the conditions where the implosion stability is provided by an axial magnetic field. The gas puff parameters optimum for the production of *K*-shell radiation had been predicted by preliminary 1D RMHD calculations. The *K*-shell radiation yield, the dimensions of the *z*-pinch radiating in the *K*-lines, and the dependence of the *K*-shell yield on the magnetic field for a gas puff with optimum parameters and an axial magnetic field are in good agreement with the predictions of the RMHD calculations.

REFERENCES

Baksht, R.B., Datsko, I.M., Fedunin, A.V., Kim, A.A., Labetsky, A.Yu., Loginov, S.V., Shishlov, A.V. & Oreshkin, V.I. (1995). The Rayleigh-Taylor instabilities and K-radiation yield for imploding gas liners. *Plasma Phys. Rep.* **21**, 907–913.

Braginskii, S.I. (1965). Transport processes in a plasma. In *Reviews of Plasma Physics* (Leontovich, M.A., Ed.), Vol. 1, p. 205. New York: Consultants Bureau.

Bud'ko, A.B., Felber, F.S., Kleev, A.I., Liberman, M.A. & Velikovich, A.L. (1989). Stability analysis of dynamic Z-pinches and theta pinches. *Phys. Fluids B* **1**, 598–607.

Cochran, F.L., Davis, J. & Velikovich, A.L. (1995). Stability and radiative performance of structured Z-pinch loads imploded on high-current pulsed power generators. *Phys. Plasmas* **2**, 2765–2772.

Coleman, P., Rauch, J., Rix, W., Thompson, J. & Wilson, R. (1997). Recent ACE-4 Z-pinch Experiments: Long implosion time argon loads, Uniform fill versus Annular shell Distributions and the Rayleigh–Taylor instability problem. In *Proc. IV Int. Conf. on Dense Z-Pinches*, AIP Conf. Proc. 409. pp.119–123.

Commisso, R.J., Apruzese, J.P., Black, D.C., Boller, J.R., Moosman, B., Mosher, D., Stepanakis, S.J., Weber, B.V. & Young, F.C. (1998). Results of radius scaling experiments and analysis of neon K-shell radiation data from an inductively driven z-pinch. *IEEE Trans. Plasma Sci.* **26**, 1068–1085.

Davis, J., Giuliani, J.L., Jr., Rogerson, J. & Thornhill, J.W. (1996). Limitation on the *K*-shell x-ray conversion efficiency of a krypton *z*-pinch plasma. In *Proc. 11th Int. Conf. on High Power Particle Beams*, pp. 709–712. (Jungwirth, K. & Ullschmied, J., Eds.). Prague, Czech Republic.

Gol'berg, S.M., Liberman, M.A. & Velikovich, A.L. (1990). Plasma compression, heating and fusion in megagauss Z-θ pinch systems. *Plasma Phys. Contr. Fusion* **32**, 319–326.

Gol'berg, S.M. & Velikovich, A.L. (1993). Snowplow mechanism and stability of imploding multicascade liner systems. In *Proc. III Int. Conf. on Dense Z-pinches*, AIP Conf. Proc. 299, pp. 42–50.

Mosher, D., Qi, N. & Krishnan, M. (1999). A two-level model for K-shell radiation scaling of the imploding z-pinch plasma radiation source. *IEEE Trans. Plasma Sci.* **26**, 1052–1061.

Oreshkin, V.I. (1994). RMHD modeling of plasma liner implosion. Preprint, HCEI SB RAS No. 4, Tomsk, Russia: High Current Electronics Institute.

Oreshkin, V.I. (1995). Implosion of plasma liners in the presence of an axial magnetic field. *Russian Phys. J.* **38**, 1203–1212.

Ratakhin, N.A. (1997). Generation of powerful X-rays in the range 7–20 keV. *Russian Phys. J.* **40**, 1198–1205.

Rudakov, L.I. (1989). Magnetically accelerated plasma shell stability. In *Proc. II Int. Conf. on Dense Z-pinches*, AIP Conf. Proc. 195. pp. 290–299.

Sorokin, S.A. & Chaikovsky, S.A. (1989). Implosion of gas-puff liners with an initial axial magnetic field. In *Proc. II Int. Conf. on Dense Z-pinches*, AIP Conf. Proc. 195. pp. 438–444.

Sorokin, S.A. & Chaikovsky, S.A. (1993). Imploding liner stabilization experiments on the SNOP-3 generator. In *Proc. III Int. Conf. on Dense Z-pinches*, AIP Conf. Proc. 299. pp. 83–92.

Sorokin, S.A. & Chaikovsky, S.A. (1996). Increase in the K-radiation yield from a gas puff. *Plasma Phys. Rep.* **22**, 897–902.

Takasugi, K., Igusa, T., Tatsumi, K. & Miyamoto, T. (2000). Control of X-ray emission from the shotgun *z*-pinch plasma. In *Proc. 13th Int. Conf. on Pulse Power Particle Beams*, pp. 470–473. (Yatsui, K. & Jiang, W., Eds.). Nagaoka, Japan.

Whitney, K.J., Thornhill, J.W., Apruzese, J.P. & Davis, J. (1990). Basic considerations for scaling Z-pinch x-ray emission with atomic number. *J. Appl. Phys.* **67**, 1725–1735.

https://doi.org/10.1017/S0263034603212143 Published online by Cambridge University Press